

Aluminium Underpotential Deposition from $\text{AlCl}_3+\text{NaCl}$ Melts and Alloy Formation with Vanadium Substrate

Niko Jovičević¹, Vesna S. Cvetković^{2,*}, Željko Kamberović¹, Tanja S. Barudžija³

¹ Faculty of Technology and Metallurgy, University of Belgrade, Karnegijeva 4, 11000 Beograd, Serbia

² Institute of Chemistry, Technology and Metallurgy, University of Belgrade, Njegoševa 12, 11000 Belgrade, Serbia, PAK 125213

³ Institute of Nuclear Sciences Vinča, University of Belgrade, P.O. Box 522, 11001 Belgrade, Serbia

*E-mail: v.cvetkovic@ihm.bg.ac.rs

Received: 23 April 2015 / Accepted: 7 September 2015 / Published: 30 September 2015

Aim of this work was to study underpotential deposition of aluminium onto polycrystalline vanadium electrode from equimolar $\text{AlCl}_3+\text{NaCl}$ melt at 473, 523 and 573 K. It was found that aluminium was deposited and incorporated into polycrystalline vanadium electrode at potentials more positive than the Al reverse potential. Applied electrochemical techniques: linear sweep voltammetry and potentiostatic deposition/galvanostatic stripping, showed clear evidence of formation of three intermetallic compounds whose presence depends on temperature and applied deposition time. Deposits were studied via scanning electron microscopy (SEM), energy dispersive spectrometry and X-ray spectroscopy (EDS and EDX), atomic force microscopy (AFM) and X-ray diffraction (XRD).

Keywords: Aluminium-Vanadium alloys, Chloroaluminate melts, Underpotential deposition, Microscopy and microanalysis techniques

1. INTRODUCTION

Studies of Al-V binary alloys are a subject of very recent investigations and availability of relevant literature is limited. Vanadium alloys have been receiving increasing attention, primarily due to their potential to meet such requirements as light weight, high strength, improved thermal stability creep resistance with promising mechanical properties at elevated temperatures. Possible applications under study are generally in nuclear-fusion reactors, coal-gasification units, gas turbines, aerospace industry, etc. [1,2]. Vanadium-aluminium alloys, due to their excellent corrosion resistance, are materials considered ideal for implant applications [3]. Because lower aluminium content alloys are

brittle and provide moderate resistance to oxidation, alloying with vanadium enhances their ductility, strength, oxidation and corrosion resistance [4-6]. For example, it is well known that single-phase V-Al alloys, produced by using conventional non-equilibrium alloying methods, exhibit greater resistance to chloride-induced pitting corrosion than pure Al metal. The mechanism of vanadium influence on structure of aluminium alloys is not completely known, but it is believed that it influences grain refining, diminishes alloy conductance and increases temperature of recrystallization [7]. One of most recent applications of Al-V binary alloys is in hydrogen membranes for fuel cells [8, 9]. Vanadium is investigated as a more cost effective alternative to palladium because it has similar hydrogen permeability performance. Alloying with 20% of aluminium should aggravate hydrogen diffusion through grain boundaries.

Production of Al-V alloys is rather difficult, vanadium is very slowly dissolved in aluminium and aluminium separates from liquid vanadium [10]. Because the normal equilibrium solubility of transition metals (including vanadium) in aluminum is rarely more than about 1 % atomic fraction (a/o), it is necessary to resort to non-equilibrium alloying methods such as melt spinning, ion implantation, reactive plasma spraying, sputter deposition, and thermal evaporation to prepare these metastable alloys. Isothermal electrodeposition from chloroaluminate melts, such as those obtained by combining anhydrous aluminum chloride with sodium chloride, mixtures of sodium chloride and potassium chloride, 1-(1-butyl)pyridinium chloride (BuPyCl), or 1-ethyl-3 methylimidazolium chloride (EtMeImCl), offers another route to these non-equilibrium materials [11].

Recent reports have again confirmed [12] that nanoscale systems, in principle, differ from bulk systems. This is especially true for a nanoscale layer of one metal (such is an underpotentially deposited monolayer from melts) in contact with another metal substrate, at moderately increased temperatures (473 to 573 K), which can lead to alloy formations.

Non-aqueous solvents that have been used successfully to electrodeposit metals and their alloys on different substrates [13-15], including aluminium and its metal alloys, are chloroaluminate molten salts [13,14,16,17] which are generated when anhydrous aluminium chloride is mixed with inorganic [13,14,18-20] or organic [13-15,17,21-23] chloride salts and then taken to the melting point. They seem to be ideal solvents for the electrodeposition of metal-aluminium alloys because they constitute a reservoir of reducible aluminium-containing species. They are excellent solvents for many metal ions, and they exhibit good intrinsic ionic conductivity.

There are records of very specific thermal formations of $\text{Al}_3\text{V}/\text{Al}_2\text{O}_3$ composites [6] or Al-V alloy [2,4,24] and very few of Al-V alloys obtained by overpotential codeposition of V and Al from organic melts – ionic liquids [11,25]. However, in literature there are no detailed studies of aluminium UPD on vanadium from inorganic melts.

We have reported on a number of alloys prepared from chloroaluminate molten salts by underpotential deposition of aluminium onto different metals [26-31] and in this article we focus on underpotential deposition (UPD) of aluminium on polycrystalline substrates of vanadium from $\text{AlCl}_3+\text{NaCl}$ equimolar melts and possible formation of intermetallic compounds with vanadium substrate.

2. EXPERIMENTAL

The electrodeposition processes were carried out in a three-electrode electrochemical cell, (made of Pyrex glass) designed for work with melts under a purified argon atmosphere and controlled by a Potentiostat/Galvanostat (Princeton Applied Research Corporation Model 273A) described earlier [26-31]. The working electrode for electrochemical experiments was 1mm diameter vanadium wire (99,99% V, Sigma-Aldrich, USA), and for surface/sub-surface analysis a 2 cm² 99,99% pure vanadium square plate. The reference electrode was 3mm diameter aluminium wire, 99,999% Al, Alfa Products, Thiokol / Ventron division, USA) in glass Luggin capillary and counter electrode was aluminium (99,999% Al) in the shape of a curved rectangular shovel (7,5 cm² active surface area). Whole cell set up (including a furnace) was placed into a transparent plastic “glove box” in order to create a moisture free atmosphere around the cell.

Surface of the aluminium reference and counter electrodes was mechanically polished, then etched in solutions of 50 vol.% HF + 15 vol. % H₂O and NH₄OH (conc. 96%) + 5 vol. % H₂O₂ and washed with triply distilled water and ethyl alcohol. The vanadium working electrodes for electrochemical experiments and for surface/sub-surface analysis after mechanical polishing were etched in (1:1 = H₂O:HNO₃) solution (stirred for 15-20 seconds) and rinsed with plenty of tap water.

Melt preparation included removal of bonded water from sodium chloride (NaCl p.a., “Merck”) [26-31] but the procedure could not be applied for drying aluminium (III) chloride (99,99% pure AlCl₃, “Aldrich Chemical Company, Inc.”). Instead, fresh, sealed bottle of anhydrous AlCl₃ was used for each experiment. Finally, the melt was subjected to pre-electrolysis between two aluminium (99,999 % Al) plates with large surface area (20cm² each) at 493-523 K with constant current density $i = 1,5 \cdot 10^{-2} \text{ A cm}^{-2}$ for 10 hours.

Linear sweep voltammetry (LSV) and potentiostatic UPD followed by galvanostatic stripping were the electrochemical techniques applied in the experiments. The first procedure with the LSV included the potential range scanned from a starting potential, E_S (usually 50 to 60 mV more negative than the open circuit potential of vanadium working electrode, (1,017 – 1,100 V measured against the aluminium reference electrode) to a final potential, E_F (0,030 – 0,050 V positive to the reversible potential of Al), followed by the return scan. In the second procedure the same potential range was scanned, but the scan was interrupted when the potential reached 0,030 – 0,050 V positive to the reversible aluminium potential; and this potential was held for $\tau_d = 1, 5$ and 10 minutes before starting the return scan. The sweep rate in both cases was 0,010 Vs⁻¹. Obtained results were recorded by Potentiostat/Galvanostat Princeton Applied Research Corporation Model 273A and an X-Y-t recorder (Hewlet Packard M7040A).

The procedure for the potentiostatic UPD followed by galvanostatic stripping included change of the working electrode potential from an initial potential, E_I (50 to 60 mV more negative to the open circuit potential of vanadium in the given melt) to a potential, E_X (30 to 50 mV more positive to aluminium equilibrium potential in the given melt), this potential was maintained for $\tau_d = 1, 5$, and 10 min whereupon the applied potential was switched off to open the electrode circuit. The electrode potential was then recorded by an XY recorder as a function of time, while a small current ($\cong 0,02 \text{ mA cm}^{-2}$) slowly stripped the aluminium from the surface of vanadium specimen. If the stripping

current was interrupted for a few seconds, the measured potential did not change significantly. This suggested that the activation overpotential which should be caused by the stripping current was negligible. This meant that the potentials measured can be considered open circuit potentials.

The samples for surface/subsurface analysis were prepared by controlled electrodeposition onto vanadium substrate from the equimolar $\text{AlCl}_3+\text{NaCl}$ melt at constant underpotential ($E_d = 0,020 - 0,100$ V vs. Al) for different time periods ($\tau_d = 60, 120$ and 240 minutes) at three different temperatures ($473, 523$ and 573 K). Then, the working electrode was removed from the melt while still under polarisation and washed in the glove box with the absolute ethyl alcohol to remove the melt residue. The sample kept without exposure to the atmosphere until subjected to surface/subsurface analysis.

The surface of the samples was examined by Scanning electron microscopy (SEM - "JEOL", model JSM-5800, Japan). In addition, atomic force microscopy (AFM) was used, with NanoScope 3D (Veeco, USA), microscope operated in contact mode under ambient conditions (silicon nitride probes with spring constant of $20-80$ N/m were used). Surface analysis was performed by Energy dispersive spectrometry (EDS - "Oxford INCA 3.2", UK), energy dispersive X-ray spectroscopy (EDX -mapping - Oxford IncaEnergy EDX). The crystal structures of alloys were characterized by XRD using (XRD - "Enraf Nonius powder diffractometer", Germany).

3. RESULTS

Fig. 1. shows linear sweep voltammograms obtained with the same sweep rate on vanadium electrodes for different cathodic end potentials. The voltammograms recorded with the same sweep rate but with different times (τ_d) spent at negative potential end of the cycle and various temperatures (T) are shown in Fig. 2. Holding potential values, E (V vs. Al) and corresponding charges (10^{-3} Acm^{-2}) under the anodic peaks recorded in the voltammograms for different deposition holding times τ_d and temperatures T , are summarized in Table 1.

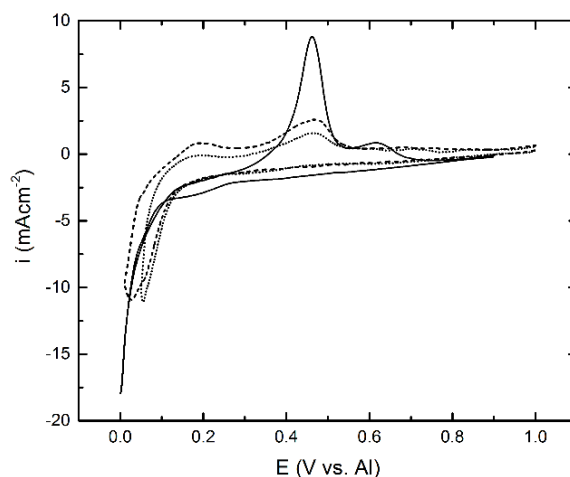


Figure 1. Linear sweep voltammograms of vanadium in equimolar $\text{AlCl}_3+\text{NaCl}$ melt; sweep rate 10 mVs^{-1} ; $T = 523$ K with following start/stop potentials: $E_i = 1,000 \text{ V} \rightarrow E_f = 0,050\text{V}$ vs. Al (dot); $E_i = 1,000 \text{ V} \rightarrow E_f = 0,010\text{V}$ (dash) vs. Al; $E_i = 1,000 \text{ V} \rightarrow E_f = 0,000\text{V}$ vs. Al (solid).

Potential vs. time diagrams of aluminium dissolution from vanadium electrodes, obtained by low-current galvanostatic stripping („open circuit measurements“) after 60 minutes UPD at different temperatures, are given in Fig. 3. Table 2 shows the potential values at the plateaux.

SEM photographs of the vanadium electrode surface obtained after a) two and b) five hours of electrode potential held at 50 mV vs. Al and 523 K are shown in Fig. 4. EDS analysis results for the same samples are presented in Fig. 5, their numerical semi-quantitative results of EDS analysis in Table 3, and EDX aluminium mapping of these surfaces in Fig. 6 a) and b).

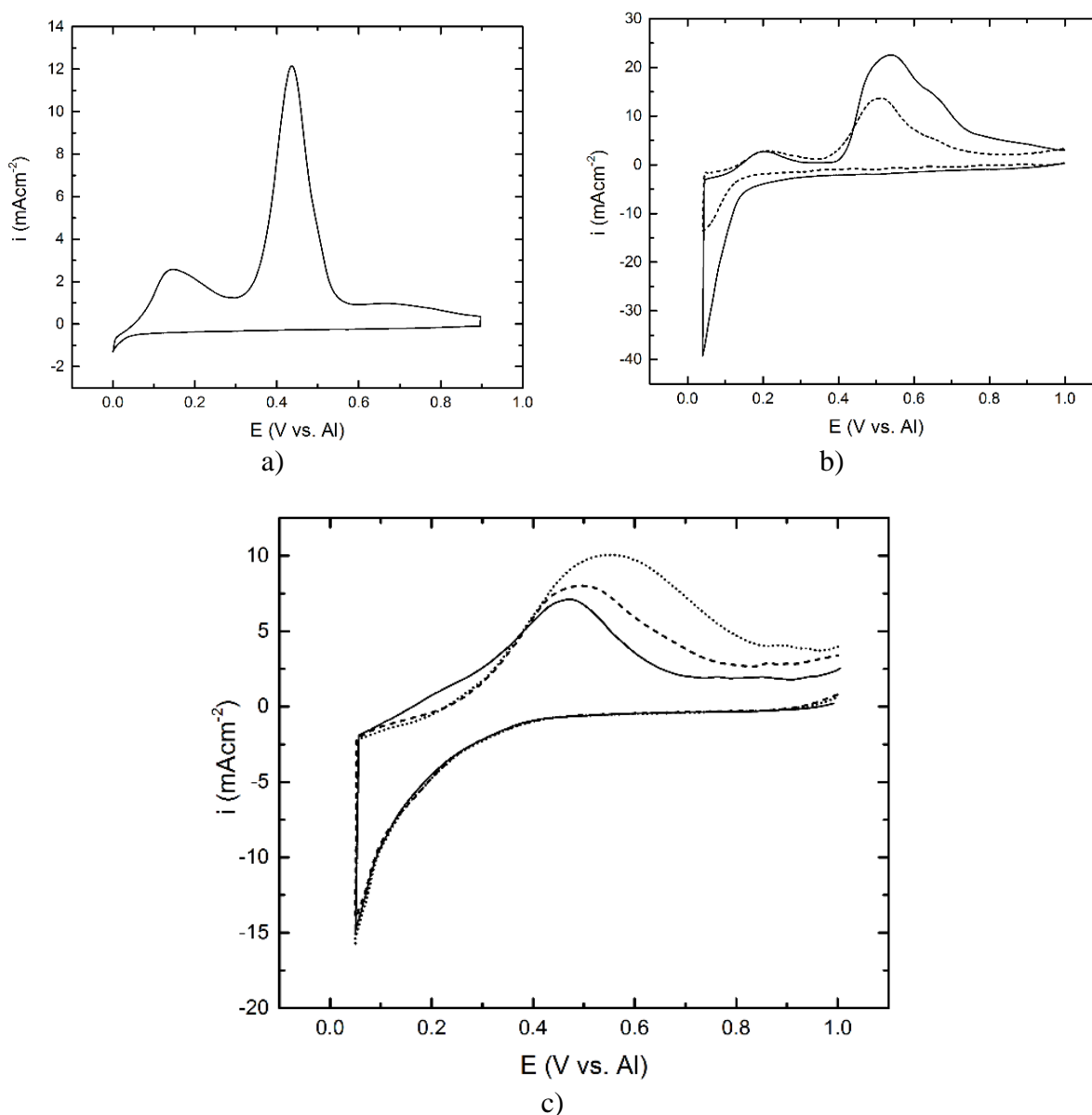


Figure 2. Linear sweep voltammograms of vanadium electrode in equimolar $\text{AlCl}_3+\text{NaCl}$ melt obtained at different times (τ_d) spent at negative potential end of the cycle; sweep rate 10 mVs^{-1} ; a) $E_i = 1,000 \text{ V} \rightarrow E_f = 0,000 \text{ V}$ vs. Al; 300s hold at 473 K; b) $E_i = 1,000 \text{ V} \rightarrow E_f = 0,040 \text{ V}$ vs. Al, 120s hold at 523 K (solid), 300s hold at 573 K (dash) and c) $E_i = 1,000 \text{ V} \rightarrow E_f = 0,050 \text{ V}$ vs. Al at 573 K, 60s (solid), 300s (dash) and 600s (dot).

Table 1. Cathodic end holding potential, E (V vs. Al) and the corresponding dissolution charge (mAs cm^{-2}) in the anodic section of voltammograms on vanadium electrodes as a function of deposition holding time τ_d (s) and temperature T (K).

Substrat	Holding time τ_d [s]	Potential E [V vs.Al]	473 K	523 K	573 K
V	120	0,040	99 mAs cm^{-2}	195 mAs cm^{-2}	267 mAs cm^{-2}
	300	0,040	182 mAs cm^{-2}	254 mAs cm^{-2}	325 mAs cm^{-2}
	600	0,040	240 mAs cm^{-2}	390 mAs cm^{-2}	411 mAs cm^{-2}

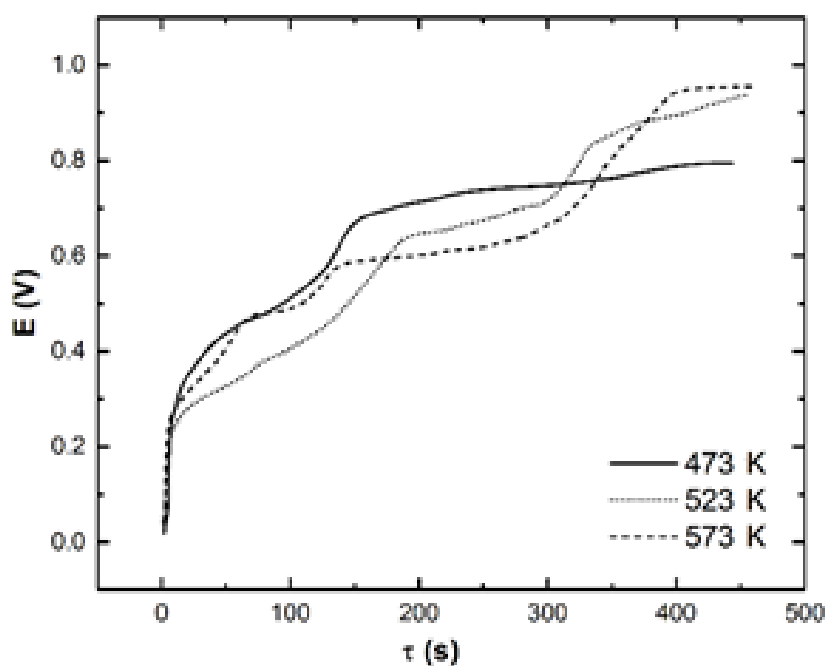


Figure 3. „Open circuit“ graphs of aluminium dissolution from vanadium electrodes in equimolar $\text{AlCl}_3+\text{NaCl}$ melt after one hour aluminium UPD at 0,020 V vs. Al; $T= 473$ K; 523 K and 573 K.

Table 2. Inflection points and corresponding E (V vs. Al) values obtained in „open circuit“ measurments after aluminium one hour UPD on vanadium in equimolar $\text{AlCl}_3+\text{NaCl}$ melt at 0,020 V vs. Al for different temperatures T (K).

T(K)	473			523			573		
Inflection Point Potential (V vs. Al)	0,166	0,273	0,382	0,133	0,270	0,530	0,260	0,480	0,560

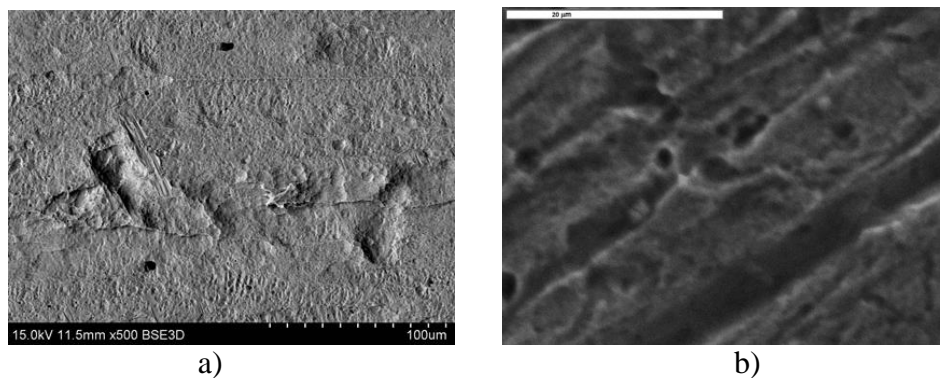


Figure 4. SEM photographs of vanadium electrode surface after: a) two hours (magnification 500x) and b) five hours (magnification 2000x) of aluminium UPD at 0,050 V vs. Al, T= 523 K.

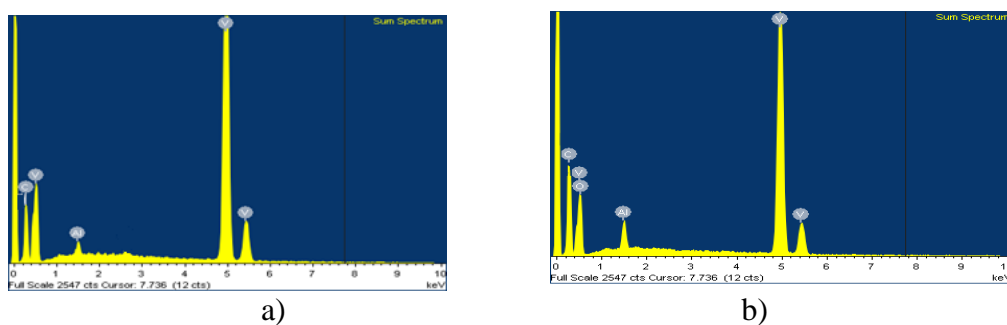


Figure 5. Characteristic EDS spectra of vanadium samples given in Fig. 4.a) and b)

Table 3. Semi-quantitative EDS analysis of the working electrode surface after two and five hours of aluminium UPD at 0,050 V vs. Al, T= 523 K (see Fig.5.a) and 5.b)).

		2 hours		5 hours	
Elmt	Spect	Elmt (%)	At.(%)	Elmt (%)	At. (%)
O K	ED	43,6	69,17	39,10	66,39
Al K	ED	2,69	2,57	5,85	4,05
V K	ED	53,71	28,26	55,05	29,56
Total		100,00	100,00	100,00	100,00

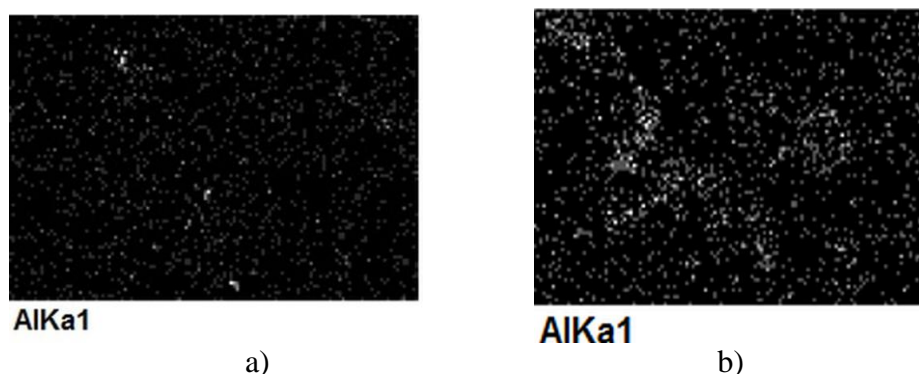


Figure 6. EDX maps of aluminium distribution after a) two and b) five hours of aluminium UPD at 0,050 V vs. Al, T= 523 K (samples from Fig. 4.) of the vanadium electrode surface

Examples of XRD patterns for vanadium electrodes taken after aluminium UPD at different temperatures and deposition times are presented in Fig. 7. The phases and their crystallographic systems identified in the deposits obtained are listed in Table 4.

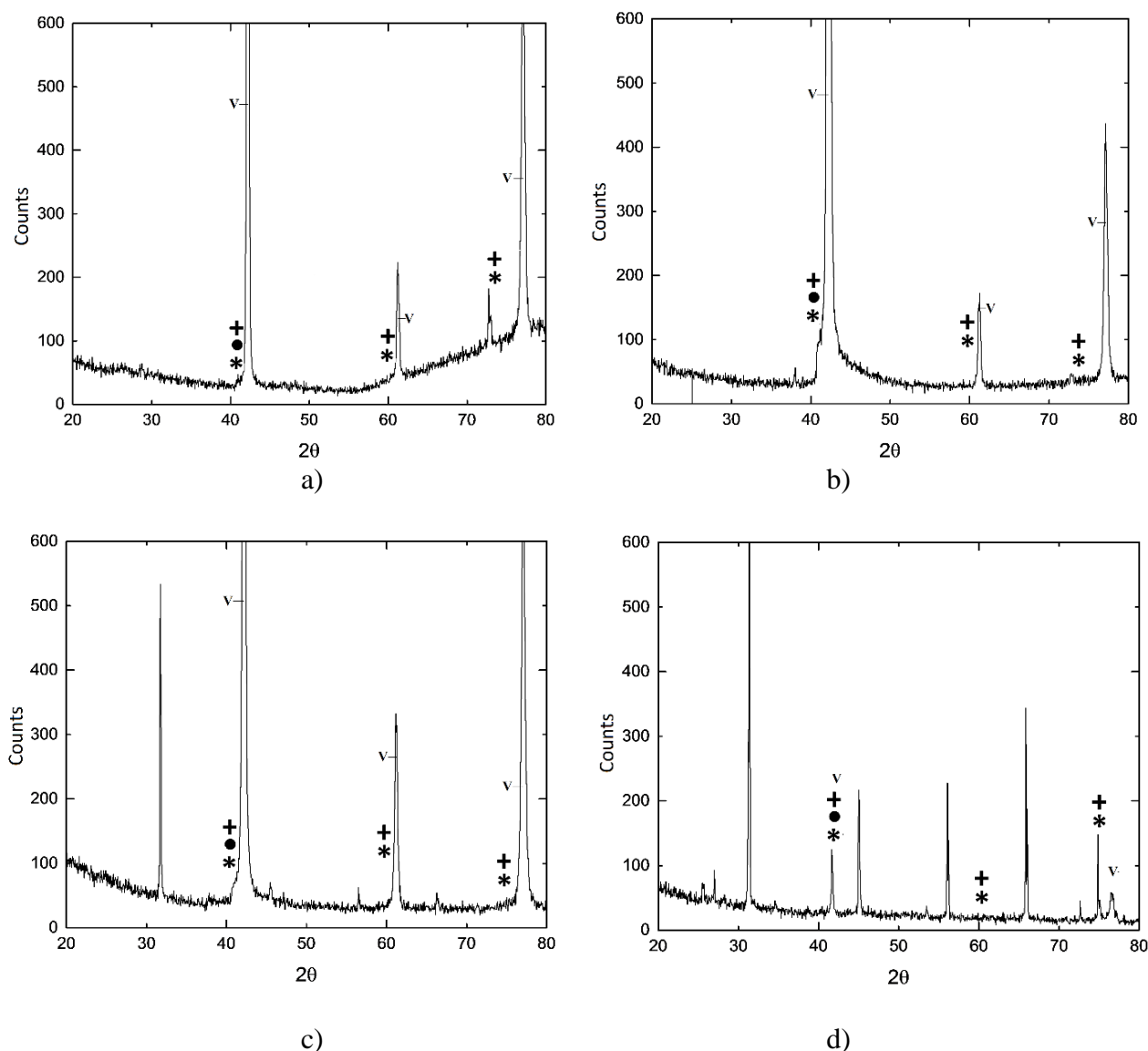


Figure 7. Diffraction patterns of vanadium electrode samples after: a) two hours of UPD at $E = 0,050$ V vs. Al from equimolar $\text{AlCl}_3 + \text{NaCl}$ melt and $T = 473$ K: (V) V, (*) AlV_3 , (●) Al_{23}V_4 , (+) Al_8V_5 ; b) two hours of UPD at $E = 0,050$ V vs. Al from equimolar $\text{AlCl}_3 + \text{NaCl}$ melt and $T = 523$ K: (V) V, (*) AlV_3 , (●) Al_{23}V_4 , (+) Al_8V_5 ; c) five hours of UPD at $E = 0,050$ V vs. Al from equimolar $\text{AlCl}_3 + \text{NaCl}$ melt and $T = 523$ K: (V) V, (*) AlV_3 , (●) Al_{23}V_4 , (+) Al_8V_5 ; d) five hours of UPD at $E = 0,050$ V vs. Al from equimolar $\text{AlCl}_3 + \text{NaCl}$ melt and $T = 573$ K: (V) V, (*) AlV_3 , (●) Al_{23}V_4 , (+) Al_8V_5 and the rest of the peaks are characteristic of AlO and Al_2O_3 .

Table 4. The phases identified by XRD on vanadium samples after aluminium UPD at different times and temperatures.

T(K)	τ_d (hour)	Identified phase	System	References
473	2	AlV ₃	cubic	[32,33]
		Al ₂₃ V ₄	hexagonal	[32,34]
		Al ₈ V ₅	cubic	[32,35]
523	2	AlV ₃	cubic	[32,33]
		Al ₂₃ V ₄	hexagonal	[32,34]
		Al ₈ V ₅	cubic	[32,35]
	5	AlV ₃	cubic	[32,33]
		Al ₂₃ V ₄	hexagonal	[32,34]
		Al ₈ V ₅	cubic	[32,35]
573	2	AlV ₃	cubic	[32,33]
		Al ₂₃ V ₄	hexagonal	[32,34]
		Al ₈ V ₅	cubic	[32,35]

Surface morphologies of the vanadium sample surface before and after aluminium underpotential deposition at 523 K for 5 hours and then analysed by AFM are presented in Fig. 8 a) and b). The surface after aluminium UPD on vanadium shows agglomerations of different sizes and a significant increase in roughness.

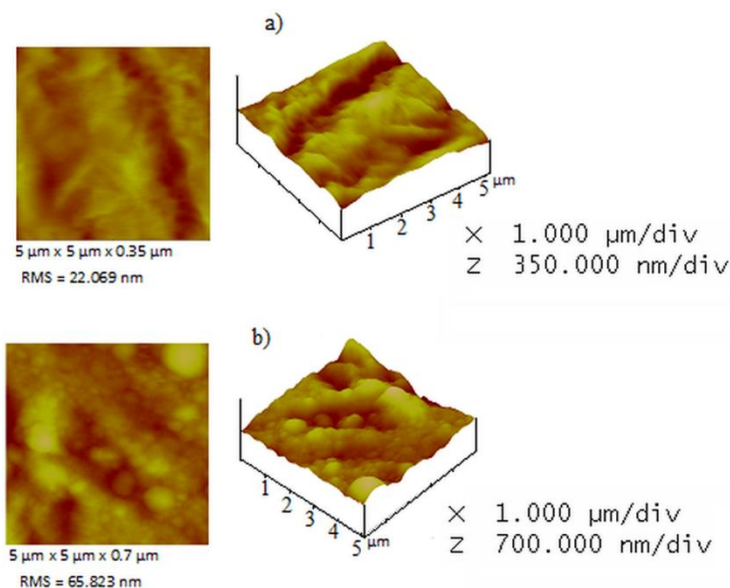


Figure 8. 2D and 3D AFM images of the vanadium surface: a) before aluminium UPD; b) after 5 hours aluminium underpotential deposition at 523 K.

4. DISCUSSION

It was established [36,37] that AlCl₄⁻ and Na⁺ are dominating ions in the melt of equimolar mixture AlCl₃+NaCl. The deposition of aluminium proceeds by reduction of AlCl₄⁻ ions and the

reversibility of this reaction establish reference potential for the electrochemical measurements in this work.

The study of aluminium underpotential deposition (UPD) on vanadium was possible because the reversible potential of the vanadium polycrystalline electrode was $1,090 \pm 0,035$ V vs. Al more in the same melt.

The cathodic current increase was not observed during linear sweep experiments with the chosen cathodic end potentials, E_d , maintained for longer times (Fig. 2). However, the anodic current peaks and the charge limited by the anodic currents increased above the charge needed for the deposition of a monolayer of aluminium [26-28]. The increase in working temperature of the system, led to an increase of the peak currents and the charges under both cathodic and anodic peaks. It would appear that the aluminium underpotential deposition after at least one aluminium monolayer completion proceeds at the rate necessary to compensate for one aluminium monolayer which entered solid state intermetallic reaction with the substrate. This dynamic quasi-equilibrium would seem to hold as long as intermetallic solid state reaction proceeds by interdiffusion of aluminium and the substrate. Different anodic dissolution peaks, then, reflect different intermetallic compounds formed during previous aluminium deposition, having different dissolution potentials [4,21,26-31,38-42] (Fig. 2.a) and b)).

The potential pulse with amplitude cathodically exceeding the potentials characteristic for the appearance of anodic peaks ($E_d = 0,030 - 0,100$ V vs. Al) followed by a quasi "open circuit" measurement of the electrode potential over time was used to obtain the dissolution characteristics of the underpotentially deposited aluminium onto and into the vanadium substrate. The "open circuit" measurements resulted in the potential-time curves exhibiting plateaux. The plateaux were the result of dissolution material being able to sustain an equilibrium potential with $AlCl_4^-$ from the melt, Fig. 3 [26-31]. The number of plateaux, Table 2, agree with the number of anodic peaks appearing on cyclic voltammograms (Table 1). The potentials of the three plateaux (Fig. 2.) agree well with the potentials of the anodic current peaks maxima in the LSV's.

Longer potentiostatic underpotential deposition caused a proportional increase in the "open circuit" dissolution time, but this did not affect the plateaux potentials. The increase in working temperature, however, increased the amount of aluminium dissolved indicating that interdiffusion of aluminium and vanadium in the solid state becomes faster at higher temperatures.

The "open circuit" measurements and the existence of the reversible (or corrosion) potentials; their temperature dependence; very similar behaviour of these potentials and the reversible aluminium potential, give strong support to the assumptions that intermetallic compounds are formed between vanadium substrate and underpotentially deposited aluminium [26-31]. It is obvious from Tables 2 and 4 that the number of plateaux observed in Fig. 3 equals the number of three two-phase regions. It was impossible to define what those three intermetallic phases were. This is not surprising, having in mind Al-V phase diagram which suggests the existence of a number of intermetallic compounds of different Al and V composition and metastable structures at temperatures below 573 K [43].

According to the literature, [44,45] UPD monolayer formation is possible if the half of work function difference ($0,5\Delta\Phi$) between the depositing metal (in this case aluminium) and the substrate (in this case vanadium) is positive. The half of work function difference for Al-V pair is positive but

very small 0,010V [46]. This would make the probability for aluminium monolayer underpotential deposition also very small. Similar relationships between theoretical predictions and experimental results, we encountered with the Al-Zn pair [31]. Here too, the linear sweep voltammograms of aluminium deposition/dissolution (Fig.1.and 2.) and low-current galvanostatic stripping measurements (Fig. 3.), clearly show that some interaction between the substrate (vanadium) and aluminium from the melt occurs at a potential positive to the potential of the aluminium reference electrode. No increase in the cathodic current during holding at the cathodic-end potential had been recorded, therefore, no nucleation barrier for alloy formation could be recognized. This should be an indication that a dynamic quasi-equilibrium is maintained at the surface by diffusion of the aluminium into the vanadium substrate. Since the aluminium–vanadium phase diagram [43] for the temperatures used shows possibility of formation of numerous intermetallic compounds, the anodic dissolution peaks could be ascribed to the aluminium from different intermetallic compounds, having, naturally, different dissolution potentials.

The results obtained with EDS and EDX clearly recognize presence of aluminium in the vanadium surface of at least 4 at. % (while vanadium was 30 at. %) after prolonged aluminium UPD (Table 3, Fig.5. and 6.). AFM analysis of the working vanadium electrode surface before and after aluminium UPD (Fig.7.) showed 2,5 times increase in surface roughness due to obvious change in morphology brought about by Al-V alloy formation. The microphotograph shown in Fig.7.a) reveals an almost flat and uniform surface of bare vanadium. The sporadic small spots of more coarse morphology could be seen, but that is probably a result of the mechanical marking during polishing. The micrograph obtained after aluminium UPD onto vanadium (Fig.7.b)) is bright in appearance and made up of small cluster of particles which are compact and uniformly cover the entire substrate. The pyramidal-shaped nodular agglomerations morphology is observed for Al-V deposit obtained from $\text{AlCl}_3 + \text{NaCl}$ melt. Another AFM image, from the smaller surface area ($5 \times 5 \mu\text{m}$), of Al deposit showed that the crystallite agglomeration was made up of smaller, nanocrystalline globular particles. The 2D image of this deposit resembles very well the morphology shown in the corresponding SEM photographs (Fig. 3.). It appears that during aluminium underpotential deposition on vanadium, under given conditions, rather thin surface alloys structures are formed.

The results obtained from XRD analysis on vanadium surfaces exposed to aluminium UPD from used melt, Fig.6., suggests that deposited aluminium under described conditions forms intermetallic compounds with vanadium, namely Al_{23}V_4 , Al_8V_5 , AlV_3 .

Solubility of vanadium in solid aluminium at 893 K is about 0,2-0,3 at.% and solubility of aluminium in vanadium is high (around 60 at.%) [43]. The Al-V intermetallic phases are structurally well characterized but the phase diagram as a whole still contains many uncertainties [43].

Interest in the possibility of AlV_3 alloy (so called A15 compound) good superconducting properties provoked numerous investigations with intermetallic phases containing around 75 at.% V. According to the Al-V phase diagram, Al_{23}V_4 (complex cubic structure) and Al_8V_5 (cubic γ brass structure) belong to solid state equilibrium phases, rich in aluminium, existing at temperatures below 960 K and 1630 K, respectively. Numerous attempts have been made to synthesize an A15 compound (AlV_3) because of its potential as a super-conducting material. Reports have been made of A15 structures formed by annealing at 373 K in quartz tubes, with lattice parameters of 0.4812

and 0.4926 nm, respectively [43]. Metallographic and microprobe analyses were made on dilute alloys heat treated for short times at temperatures between 773 and 1013 K. It was concluded that only Al_3V and Al_6V (Al_{23}V_4) are equilibrium phases, and that Al_{21}V_2 appears only as a metastable transition phase [5,43]. Hexagonal β AlV_3 , with $a = 0.7070$ and $c = 0.9565$ nm, was reported to form under pressures greater than 30 kbar and above 1773 K and tetragonal α AlV_3 , with $a = 0.6167$ and $c = 0.9481$ nm, appeared at lower temperatures and pressures [47]. Hexagonal β AlV_3 , with $a = 0.7070$ and $c = 0.9565$ nm, was reported to form under pressures greater than 30 kbar and above 1773 K and tetragonal α AlV_3 , with $a = 0.6167$ and $c = 0.9481$ nm, appeared at lower temperatures and pressures [47].

Some authors [10] consider that Al_{45}V_7 and Al_{23}V_4 (around 24 at. % of vanadium) alloys can be obtained only by diffusion mechanism, and not by casting. They suggest that the intermediary phase Al_3V is isomorphic with Al_8V_5 and has significant range of solubility of aluminium up to 1633 K. Pronounced tendency of aluminium and vanadium to build superlattice formations in alloys was also observed.

Annealing at temperatures below about 973 K caused interdiffusion between V and Al thin layers results mainly in a solid-solution of Al in V [48]. After annealing for 1 hour at a temperature higher than about 973 K, several compounds were found to form by the reactions between the V-Al solid solution including Al_5 and some unidentified phase made with oxides [48]. V_5Al_8 and V_3Al intermetallics have been formed by interdiffusion, by annealing of sputtered V/Al-multilayers at 973 K in vacuum; sapphire (102) was used as substrate.

5. CONCLUSIONS

Electrochemical techniques revealed underpotential deposition of aluminium from equimolar $\text{AlCl}_3 + \text{NaCl}$ melt on polycrystalline vanadium substrate at temperatures 473 K, 523 K and 573 K. The observed aluminium underpotential deposition results in the formation of surface intermetallic compounds by interdiffusion of thin Al deposit and V substrate. The constant-potential regions measured during the low-current stripping corresponded to the coexistence of four pairs of the metallic-intermetallic phases.

The deposits were studied by scanning electron microscopy (SEM), energy dispersive spectrometry and X-ray spectroscopy (EDS and EDX), atomic force microscopy (AFM) and X-ray diffraction (XRD) which confirmed aluminium UPD on vanadium and Al-V alloys formation. Three intermetallic compounds were identified as Al_{23}V_4 ; Al_8V_5 . AlV_3 .

The results suggest new possibilities of Al-V alloys formation (including famous AlV_3) using lower temperatures via a better controlled processes.

ACKNOWLEDGEMENT

This work was supported by Ministry for Education and Science – Republic of Serbia under contract No. ON 176020

References

1. J. G. Keller and D. L. Douglas, *Oxid. Met.*, 36 (5) (1991) 439.
2. H. Lewalter, W. Bock and B. O. Kolbesen, *Anal. Bioanal. Chem.*, 374 (2002) 724.
3. C. G. Nava-Dino, C. López-Meléndez, R. G. Bautista-Margulis, M. A. Neri-Flores, J. G. Chacón Nava, S. D de la Torre, J. G. Gonzalez-Rodriguez and A. Martínez-Villafañe, *Int. J. Electrochem. Sci.*, 7 (2012) 2389.
4. V. R. V. Ramanan, D. J. Skinner and M. S. Zedalis, *Mater. Sci. Eng.*, A 134 (1991) 912.
5. B. Grushko and T. Y. Velikanova, *Journal Alloys Compd.*, 367 (2004) 58.
6. N. Yazdian, F. Karimzadeh and M. H. Enayati, *Advanced Powder Technology*, 24 (2013) 106.
7. S. Boczkal, M. Lech-Grega and J. Morgiel, in *Light Metals*, ed. J. Grandfield, John Wiley & Sons, Inc., Hoboken, New York (2014).
8. M. D. Dolan, M. E. Kellam, K. G. McLennan, D. Liang and G. Song, 2013, *Int. J Hydrogen Energ.*, 39 (33) (2014) 19009.
9. K. Kim and T. Hong, *Trans. of the Korean Hydrogen and New Energy Society*, 22 (4) (2011. 8) 458.
10. D. J. Kenney, H. A. Wilhelm and O. N. Carlson, *Aluminium-Vanadium System*, ISC-353, Ames Laboratory, United State Atomic Energy Commission, Oak Ridge, Tennessee, (1953).
11. T. Tsuda and C. L. Hussey, *J. Min. Met.*, 39 (1 - 2) B (2003) 3.
12. P. Liddicoat, X. Liao, Y. Zhao, Y. Zhu, M. Murashkin, E. Lavernia, R. Valiev and S. Ringer, *Nat. Commun.*, 1 (63) (2010) 1.
13. R. E. Watson and M. Weinert, *Physical review B*, 58 (10) (1998) 5981.
14. G. R. Stafford and C. L. Hussey, in *Advances in Electrochemical Science and Engineering*, Vol.7, (ed. R. C. Alkire and D. M. Kolb), Wiley-VCH Verlag GmbH, New York (2001).
15. W. Simka, D. Puszczuk and G. Nawrat, *Electrochim. Acta*, 54 (23) (2009) 5307.
16. C. L. Hussey, in *Electroanalytical Chemistry in Molten Salts*, (ed. P.T. Kissinger and W. R. Heinmann), Marsel Dekker, New York (1996).
17. S. Geetha and D. C. Trivedi, *Bulletin of electrochemistry*, 19 (5/6) 2003 37.
18. V. D. Jović and J. N. Jovičević, *J. Appl. Electrochem.*, 19 (2) (1989) 275.
19. G. Mamantov, C. L. Hussey and R. Marassi, in *Techniques for characterization of electrodes and electrochemical processes*, (Ed. R. Varma and J. R. Selman), John Wiley and Sons, New York (1991).
20. M. Jafarian, F. Gobal, I. Danaee, M. G. Mahjani, *Electrochim. Acta*, 52 (17) (2007) 5437.
21. C. Scordilis-Kelley, J. Fuller and R. T. Carlin, *J. Electrochem. Soc.*, 139 (3) (1992) 694.
22. T. Tsuda, C. L. Hussey and G. R. Stafford, *J. Electrochem. Soc.*, 152 (9) (2005) C620.
23. S. I. Hsiu, C. C. Tai and I. W. Sun, *Electrochim. Acta*, 51 (13) (2006) 2607.
24. M. Fetcenko, *Preparation of Vanadium rich Hydrogen storage alloy materials*, US Patent, No. 5,002,703 (1991).
25. T. Tetsuya and C. L. Hussey, *Symposium on Magnetic Materials, Processes, and Devices VII and Electrodeposition of Alloys*, 202nd Meeting of the Electrochemical Society, Solt Lake City, Utah, October 20-24 (2002).
26. B. S. Radović, R. A.H. Edwards and J. N. Jovičević, *J. Electroanal. Chem.*, 428 (1-2) (1997) 113.
27. B. S. Radović, R. A. H. Edwards, V. S. Cvetković and J. N. Jovičević, *Kovove mater.*, 48(1) (2010) 55.
28. B. S. Radović, V. S. Cvetković, R. A. H. Edwards and J. N. Jovičević, *Kovove mater.*, 48 (3) (2010) 159.
29. B. S. Radović, V. S. Cvetković, R. A. H. Edwards and J. N. Jovičević, *Int. J. Mat. Res.*, 102 (1) (2011) 59.
30. N. Jovičević, V. S. Cvetković, Ž. J. Kamberović and J. N. Jovičević, *Metall. Mater. Trans. B*, 44 (1) (2013) 106.

31. N. Jovičević, V. S. Cvetković, Ž. J. Kamberović and J. N. Jovičević, *Int. J. Electrochem. Sci.*, 7 (2012) 10380.
32. The International Centre for Diffraction Data (ICDD), PDF-2, Release 2003.
33. The International Centre for Diffraction Data (ICDD), PDF-2, Entry 000-007-0360, Release 2003.
34. The International Centre for Diffraction Data (ICDD), PDF-2, Entry 030-065-2085, Release 2003.
35. The International Centre for Diffraction Data (ICDD), PDF-2, Entry 030-065-5142, Release 2003.
36. L. G. Boxal, H. L. Jones and R. A. Osteryoung, *J. Electrochem. Soc.*, 20 (1973) 223.
37. A. A. Fannin, L. A. King and D. W. Seegmiller, *J. Electrochem. Soc.*, 119 (1972) 801.
38. A. Bewick, J. N. Jovičević and B. Thomas, *Faraday Symposia of the Chem. Soc.*, 12 (1977) 24.
39. H. Bort, K. Jüttner, W.J. Lorenz and G. Staikov, *Electrochim. Acta*, 28 (1983) 993.
40. E. Schmidt and H. Siegenthaler, *J. Electroanal. Chem.*, 150 (1983) 59.
41. R. Vidu, N. Hirai and S. Hara, *Phys. Chem. Chem. Phys.*, 3(16) (2001) 3320.
42. R. Vidu and S. Hara, *Surface Sci.*, 452(1-3) (2000) 229.
43. J. L. Murray, *Bulletin of Alloy Phase Diagrams*, 10 (1989) 4.
44. H. Gerischer, D. M. Kolb and M. Przasnyski, *Surf. Sci.*, 43 (1974) 662.
45. D. M. Kolb, M. Przasnyski and H. Gerischer, *J. Electroanal. Chem.*, 54 (1974).
46. CRC Handbook of Chemistry and Physics, CRC Press, INC, Boca Raton (2002).
47. J. M. Leger, H. T. Hall, *J. Less.Common Met.*, 32 (1973) 181.
48. N. Hayashi, K. Morii and Y. Nakayama, *Materials Transactions*, 32 (3) (1991) 285.

© 2015 The Authors. Published by ESG (www.electrochemsci.org). This article is an open access article distributed under the terms and conditions of the Creative Commons Attribution license (<http://creativecommons.org/licenses/by/4.0/>).